COBEM 2021 26th International Congress of Mechanical Engineering
November 22-26, 2021, Virtual Congress, Brazil

COB-2021-2004
FIRST-ORDER CONSTRUCT OF A MINERAL CARBONATION SYSTEM FOR POST-COMBUSTION CARBON CAPTURE

Claudia Luiza Manfredi Gasparovic
George Stanescu
Marcelo Risso Errera
Federal University of Paraná, Graduate Program of Environmental Engineering (PPGEA), Av. Cel. Francisco H. dos Santos, Curitiba, 81530-000, Brasil
claudiagasparovicea@gmail.com
stanescu@ufpr.br
errera@ufpr.br

Abstract. *This paper aims to address the constructal design of a Mineral Carbonation reactor for CO_2 capture. This will be achieved by applying the constructal method to the process' degrees of freedom of the geometric scales of the first construct, and studying the effect on merit figures such as rate of CO_2 captured and pressure losses under global restrictions such as fixed reactor and substract volumes, using analytical and numerical models of the process. We formulate the Constructal problem of the First Construct by identifying that for the restriction of fixed $\dot{m}_1$, A1, and W, the construct presents four degrees of freedom (DoF). We choose to address these DoF as the apparent porosity (φ_1), the aspect ratio of the porous bed (L_0/H_s), the width ratio of the gas channels (d_1/d_0), and the number of elemental volumes in the construct (n). A numerical simulation for the designed first construct was then performed on COMSOL Multiphysics®, for pressure, velocity and concentration fields. Numerical results of pressure and velocity converge to analytical results. Results for the multi-scale design show that it is possible to carry out the process with low pressure drops by working with the design guidelines provided by the Constructal method.*

Keywords: *carbon capture, greenhouse gases, constructal design, mineral carbonation*

1. INTRODUCTION

The concern with global warning has motivated research work regarding the control and reduction of anthropogenic emissions of greenhouse gases (Cecchi *et al.* 2017; Leung *et al.*, 2014), especially of carbon dioxide (CO_2), which is considered the main responsible gas for the phenomenon (Mazzella et al., 2016; Siriruang et al., 2016).

Among the options for mitigation, post-combustion carbon capture has been considered crucial due to the great amount of point emissions of CO_2 that occurs in the energy generation chain (Ukwattage et al., 2015). The processes of Mineral Carbonation (MC), in which carbon in gaseous form (CO_2) is converted to stable solid carbonates (Ukwattage et al., 2017) has shown to be an interesting solution for the disposal of CO2 in the long term, due to the stability of the produced products (Muriithi *et al.*, 2013), thus being the safest way of storing CO_2 (Cecchi *et al.*, 2017).

Despite its advantages, there are technical challenges that need to be overcome in order to scale-up the technology, such as energy efficiency and achieving sufficiently fast kinetics. Design of devices need to address these challenges to make equipment compatible with flue gas emissions flow rate. Better designs can be achieved by the Constructal approach, which guides the designer to the evolutionary path of configurations that lead to increase in the flow access of the system's currents. A better reactor design is one that shows maximum mass transfer over time into a fixed reactor space with minimum energy expenditure.

In the MC system, CO_2 from the gas feeding stream permeates a porous capturing media partially saturated with water. The permeated CO_2 dissolves in the liquid phase and reacts with the alkali species dissolved from the substract via a series of reactions of the carbonate system. The gas, now lower in CO_2 content, exits the porous bed through a collecting channel. Thus each porous bed will have two adjacent and parallel channels, one with the purpose of feeding gas, the other collecting gas, alternately. The capturing media considered is calcium hydroxide $Ca(OH)_2$.

A mathematical model for the process was built based on the work of Rivera-Alvarez and Bejan (2003), Ishida and Maekawa (2000), Jeong *et al.*, (2019) and Papadakis *et al.*, (1989). The model considers molar balances, equilibrium in the gas-liquid interface via Henry's Law, chemical equilibrium of the carbonate system, chemical kinetics for the carbonation reaction, mass transport in the porous medium and fluid flow in free and porous media (Navier-Stokes and Darcy equations, respectively).

This paper aims to address the Constructal design of a MC reactor for CO_2 capture. This will be achieved by applying the Constructal method to the process' degrees of freedom of the geometric scales of the first construct and studying their

effect on merit figures such as amount of CO_2 captured averaged over time and pressure losses, under global restrictions such as a fixed reactor volume. This analysis continues from previous results of temporal scales of the process and number of elemental volumes in the assembly (Gasparovic et al., 2019, 2020) and is based on Rivera-Alvarez and Bejan (2003) and Malley-Ernewein and Lorente (2019).

2. CONFIGURATION AND MODEL

According to the Constructal method, we start by identifying the "elemental volume" (e.v.) of the process, i.e. the smallest finite-size unit that is able to carry out the target process. It consists of one porous bed of dimensions L_0 (length) and d_s (thickness), with a feeding channel in between them, and half of a collecting channel on either (top or bottom) end, both of dimensions L_0 (length) and d_0 (thickness), with total height $H_0 = d_s + 2d_0$. An assembly of n elemental volumes, plus one feeding and one collecting channel, constitutes the First Construct of the process, as illustrated in Figure 1.

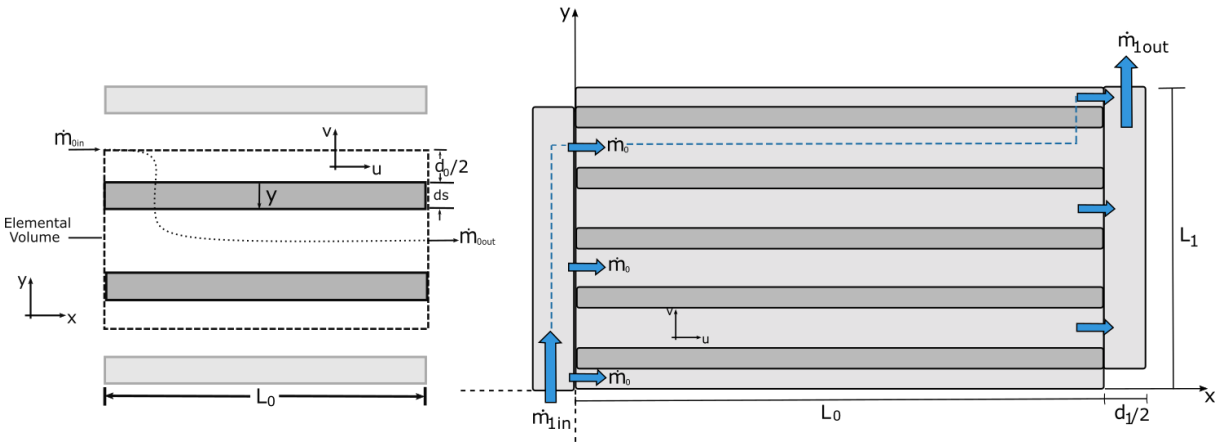

Figure 1. Elemental volume and first construct.

The global size of the first construct (A_1) is fixed, $V_1 \sim (L_0 + d_1) W L_1$ where L_1 is the total thickness of the stack, which is of order $L_1 = nH_0$. . The volume of substract V_s is dictated by the apparent porosity $\varphi, = 1 - (V_s/V_1)$ and has a total thickness of $H_s = nd_s$. Note that dimensions along direction of flow in the channels are denoted as length (Li), and across direction of flow are described as thickness (di) and height (Hi), with index i indicating the level of assembly.

The assembly is fed a fixed total gas mixture stream $\dot{m}_1$, where the stream passing in each channel is $\dot{m}_0 = \frac{2\dot{m}_1}{(n+1)}$, and the stream passing in each bed is $\dot{m}_s = \dot{m}_0/2$. The exhaust ducts have the same geometry as the feeding ducts.

2.1 Mechanism and assumptions

The overall reaction for CO_2 capture using $Ca(OH)_2$ aqueous solution is expressed as Eq. (1) (Han et al., 2011):

$$Ca(OH)_{2(s)} + CO_{2(g)} \leftrightarrow CaCO_{3(s)} + H_2O_{(l)}, \quad (1)$$

The main mechanisms during the carbonation period are summarized below (Jeong *et al.*, 2019):

$$H_2O \leftrightarrow H^+ + OH^-, \quad (2)$$

$$H_2CO_3 \rightarrow H^+ + HCO_3^- \leftrightarrow 2H^+ + CO_3^{-2}, \quad (3)$$

$$Ca(OH)_2 \rightarrow Ca^{2+} + OH^-, \quad (4)$$

$$Ca^{2+} + CO_3^{-2} \leftrightarrow CaCO_3, \quad (5)$$

The following assumptions are adopted in the modeling of the reaction system:

1. The reaction takes place in the liquid phase of a monodisperse porous media reactor of semi-continuous operation regime (continuous in relation with the gas phase and batch for capturing media) (GÓMEZ-DIAZ; NAVAZA; SANJURJO, 2006), at close to ambient conditions of temperature and pressure, and with low humidity. The reactor is considered to be in isothermal conditions.

2. According to the film model, a stagnant film is assumed at both sides of the interface gas-liquid and all resistance to mass transport is located in these two films. This means that concentration gradients will only develop in these films. (HOSTEN; 1983).

3. It is further assumed that no resistance to transport occurs at the interface itself, such that the interface concentration of the gaseous component in the solution is related to the interfacial partial pressure by Henry's Law:

$$[CO_2]_d = HRTP_{co_{2g}}, \tag{6}$$

In which H is Henry's constant, equal to 3.3×10^{-4} mol/m³.Pa (Sander 2015). The liquid film is thin enough that CO_2 concentration is uniform in the liquid bulk.

4. Reactions represented by Eqs.(2-4) occur instantaneously or in a time scale negligible in comparison to the rate of reaction of Eq. (5). This assumption is in accordance to Jeong *et al.*, (2019), Ishida and Maekawa (2000) and Mitchell (2010) who carried out an asymptotic analysis of the process, which allowed to capture the behavior of the reaction system and the determining time scales for the reaction rates. The author concluded that, considering good mixture conditions, the remaining reactions occur rapidly, while the precipitation reaction is slow and would be limiting for the overall rate.

5. As a consequence of 4, concentrations of species of the carbonate system are given by the chemical equilibrium relations of the carbonate system. According to Snoeyink and Jenkins (1980), this equilibrium for the carbonate species is given by:

$$[CO_3^{2-}] = \alpha_2[CO_2]_d, \tag{7}$$

$$\alpha_2 = \frac{K_a K_b}{[H^+]^2 + K_a[H^+] + K_a K_b} \tag{8}$$

In which K_i is the equilibrium constant for each dissociation. We consider $K_w = 1{,}00x10^{-14}$, $K_a = 10^{-6,3}$ and $K_b = 10^{-10,3}$ at 25ºC (Snoeyink and Jenkins 1980).

6.The reaction rate of the precipitation reaction considers a first-order reaction with respect to the concentration of species Ca^{2+} and CO_3^{2-}, with rate constant equal to 2.08 L.mol^{-1}.s^{-1}, as described by Ishida and Maekawa (2000) (supported by the similar value of 2 L.mol^{-1}.s^{-1} described by Mitchell (2010)).

$$r_c = \frac{d}{dt}[CaCO_3] = k[Ca^{2+}][CO_3^{2-}], \tag{9}$$

7. Moreover, the reaction described in Eq. (9) is considered irreversible due to calcium carbonate being practically insoluble in water at pH above 9 (Pan et al., 2012). The pH of the reaction is expected to be maintained above this value as explained in assumption 9. Thus, the backwards reaction rate is not considered in the model.

8.Furthermore, the reaction described in Eq. (9) is considered to be of pseudo-first order with respect to the carbon dioxide species, a limiting case of the film theory in which, according to Hosten (1983), the reaction is first order with respect to the gaseous component, and the concentration of the other species is uniform throughout the film. This assumption is valid for cases of low humidity in which a sharp reaction front is not formed, in accordance to Jeong *et al.*, (2019) and Papadakis *et al.*, (1989) and will be further justified in the section describing the molar balance of calcium hydroxide. In other words, the dissolution rate of $Ca(OH)_2$ is equal to the rate of formation of calcium carbonate, and thus, the concentration of the Ca^{2+} species in the liquid film are is maintained at the solubility limit.

9. As a consequence of 8 and of the equilibrium relations of ions Ca^{2+} and OH^-, concentration of ion hydroxyl is also maintained at the level of equilibrium of $Ca(OH)_2$ dissolution, and so, pH of the solution is maintained at a constant level (calculated from Kps as equal to 12.37).

10. Water volume fraction is considered constant regardless of the amount of H_2O produced or consumed by the chemical reactions (Papadakis et al., 1989).

11. Modeling considers an ideal gas for the gas mixture, of approximately constant viscosity and Darcy velocity (given the low initial concentration of CO_2 in the gas, so that the change in mass flow rate due to carbonation is negligible).

12. Permeability, porosity of the medium are considered as approximately constant (given that the conversion rate at the end of process is low, due to excess of capturing material).

2.2 Molar balance of calcium hydroxide

The molar balance of solid $Ca(OH)_2$(s) can be written as following (Jeong *et al.*, 2019; Papadakis *et al.*, 1989):

$$\frac{d[Ca(OH)_{2(s)}]_{bed}}{dt} = -r_D, \tag{10}$$

Where r_D is the sink term due to solid hydroxide dissolution rate. The initial concentration of solid calcium hydroxide in the bed is given by:

$$\left[Ca(OH)_{2(aq)}\right]_{bed,0} = \frac{(1-\varepsilon)}{V_{CH}}, \tag{11}$$

Where V_{CH} is the molar volume of $Ca(OH)_2$ in m³/mol.

In aqueous solution $Ca(OH)_{2(aq)}$, OH^- diffuses from the regions with higher concentration of OH- to those with lower concentrations. It can be handled by means of the diffusion coefficient $D_{e,Ca(OH)_{2(aq)}}$ according to Jeong *et al.*, (2019) and Papadakis *et al.*, (1989)**.** This diffusion usually takes place at the aqueous phases of the pores.

According to Papadakis *et al.*, (1989), this diffusion term can be neglected in good approximation even for normal exposure (not accelerated) conditions.

The mass balance of dissolved $Ca(OH)_{2(aq)}$ is given by:

$$\frac{d[Ca(OH)_{2(aq)}]_{bed}}{dt} = (-\mathrm{Div}(-D_{e,Ca(OH)_{2(aq)}}\nabla(\left[Ca(OH)_{2(aq)}\right]_{bed})) - r_c + r_D)\frac{1}{\varepsilon f_w}, \tag{12}$$

Where ε is bed porosity, f_w the volume fraction of aqueous film at the walls of the pores (ratio of film volume to pore volume), andr_c the carbonation reaction rate.

As a consequence of neglecting the diffusion term, and as follows from equilibrium relations, according to Jeong *et al.*, (2019) and Papadakis *et al.*, (1989) this gives rise to the equality of r_c and r_D, thus simplifying the balance equations.

2.3 Molar balance of carbon dioxide

The balance of gaseous carbon dioxide in the porous bed is given by:

$$\frac{d[CO_2]_{g,bed}}{dt} = \frac{1}{\varepsilon(1-f_w)}[\nabla\cdot(\boldsymbol{v}[CO_2]_g) + \nabla\cdot\left(\frac{D_m}{\varepsilon}\nabla[CO_2]\right)] - r_{D_{CO_2}}, \tag{13}$$

In which Darcy $\boldsymbol{v}$ is velocity in the porous media, $[CO_2]_g$ the CO_2 concentration in gas, $r_{D_{CO_2}}$ is the dissolution rate of $CO_{2(g)}$ in the liquid film, and D_m the carbon dioxide diffusivity coeficients in porous media, given by (Li *et al.*, 2017):

$$D_m = \frac{\varepsilon}{\tau}D, \tag{14}$$

In which in which *D* is the diffusivity in the air, equal to 1,97×10-9 (m²/s) (Frank *et al.*, 1996) and τ the tortuosity, given by $\varepsilon^{1/3}$ according to (Millignton and Quirk 1959).

The balance of aqueous carbon dioxide, is given by, considering isotropic dispersion in the liquid medium:

$$\frac{d[CO_2]_{aq,bed}}{dt} = [-r_c + r_{D_{CO_2}}\frac{1}{\varepsilon f_w} + (-(-D_{e,CO_{2aq}}\nabla^2(\left[CO_{2aq}\right]_{bed}))\ \ ], \tag{15}$$

Where, assuming that the diffusion term is large enough that gradients in concentration of aqueous CO_2 in the liquid film are negligible, and that variations in time for CO_2 concentration in the liquid are negligible, due to the equilibrium of gaseous-liquid interface and stationary assumption for gas flow, gives rise to the equality of $r_c and\ r_{D_{CO_2}}$.

The carbonation reaction rate can be expressed as (9). Considering equilibrium relations expressed in Eq. (7) and Henry's Law, Eq. (6) can be rewritten as:

$$r_c = \frac{d}{dt}[CaCO_3] = k[Ca^{2+}]a_2[CO_2]_{g,bed}HRT\ , \tag{16}$$

Where we can substitute the concentration of calcium by:

$$[Ca^{2+}] \cong S_{Ca^{2+}}, \tag{17}$$

Where $S_{Ca^{2+}}$ is the solubility limit of the calcium species. Finally, we can write Eq. (15) as:

$$\frac{d[CO_2]_{g,bed}}{dt} = \frac{1}{\varepsilon(1-f_w)}\left[\nabla\cdot(\boldsymbol{v}[CO_2]_g) + \nabla\cdot\left(\frac{D_m}{\varepsilon}\nabla[CO_2]\right)\right] - kS_{Ca^{2+}}[CO_2]_{g,bed}HRT\frac{\varepsilon f_w}{\varepsilon(1-f_w)}, \tag{18}$$

2.3.1 Fluid flow model

Fluid flow in porous media was modeled with Darcy equation, which for isotropic media can be written (Nield and Bejan 2017):

$$\boldsymbol{v} = \frac{-K}{\mu}\nabla \boldsymbol{P}, \tag{19}$$

In which $\boldsymbol{v}$ is the Darcy velocity, K the permeability, μ the dynamic viscosity, and ∇P the pressure gradient.

For the gas channel, fluid flow is described by Navier-Stokes equations, considering incompressible and constant viscosity flow (Nield and Bejan 2017):

$$\rho \frac{d\boldsymbol{U}}{dt} + \rho(\boldsymbol{U} \cdot \nabla)\boldsymbol{U} = -\nabla p + \mu \nabla^2 \boldsymbol{U}, \tag{20}$$

In which $\boldsymbol{U}$ is the fluid velocity in the gas channel, and ρ is fluid density.

3. CONSTRUCTAL DESIGN UNDER THE STATIONARY REGIME

We start the study by working with simplifying hypothesis for the reaction model, which will later be relaxed. According to the Constructal Method, the fundamental parts of a flow system are first identified: what flows, what are the degrees of freedom for design, and what are the restrictions the system is subject to. We then vary each of the degrees of freedom, study the effects it has in the system, select the best performing result, and repeat the process considering the previous results. Here, we wish to provide better access to the capturing bed to the reacting flow containing CO2. Having established the degrees of freedom, restrictions, and goal, we then identify the compromises that present opportunities for design. The degrees of freedom relate to the temporal and geometry scales of the elemental volume and will be further explained.

We formulate the Constructal problem of the First Construct by identifying that for the restriction of fixed $\dot{m}_1$, A_1, and W, the construct presents four degrees of freedom (DoF). We choose to address these DoF as the apparent porosity (φ_t), the aspect ratio of the porous bed (L_0/H_s), the width ratio of the gas channels (d_1/d_0), and the number of elemental volumes in the construct (n).

To increase flow access of the first construct means to minimize the pumping power required to drive $\dot{m}_1$ through the construct, which is the same as minimizing the overall pressure drop ΔP between the inlet and outlet of the stream. Thus we start by studying analytically the effects of these DoF in the pressure losses and conversion of the system.

The system was studied under the conditions presented in Table 1. The concentration of CO2 in exhaust gases was determined according to stoichiometric relations for combustion of methane. The stoichiometric combustion reaction of CH4 with air is given by (Borgnakke and Sonntag 2013):

$$CH_4 + 2O_2 + 2(3.76)N_2 \rightarrow CO_2 + 2H_2O + 7.52N_2, \tag{21}$$

Which means that the molar fraction of CO_2 in exhaust gases (dry basis) is of 0.117.

Table 1. Conditions and parameters employed

Parameter	**Value**
Area of first construct (A_1)	0,25 m²
Width of first construct (W)	0,1 m
Volumetric flow rate in first construct (Q_1)	50 L/min
Viscosity of gases (μ_g)	1.825e-5 kg/(m.s)
Density of gases (ρ_g)	1.204 kg/m³
Permeability of porous medium (K)	10^{-10}
Temperature of gases (T)	353 K

3.1 Pressure losses

ΔP has three components: the pressure drops in the L direction of the elemental volume (ΔP_0), the pressure drops in the L_1 direction (ΔP_1), and the pressure drops in the porous bed (ΔP_s).

Pressure losses were calculated analytically, for the parameters presented in Table 1. Each term of the pressure drops can be estimated analytically as (Bejan and Lorente 2008):

$$\Delta P_0 \sim \frac{48\mu U_0}{(D_{h0})^2} \tag{22}$$

$$\Delta P_1 \sim \frac{48\mu U_1}{(D_{h1})^2} \tag{23}$$

$$\Delta P_s \sim \frac{v\mu d_s}{K} \tag{24}$$

3.1.1 Apparent porosity

Figure 2 shows how total pressure losses change when the number of elements in the construct also vary, and how the configuration of the first construct varies for both degrees of freedom.

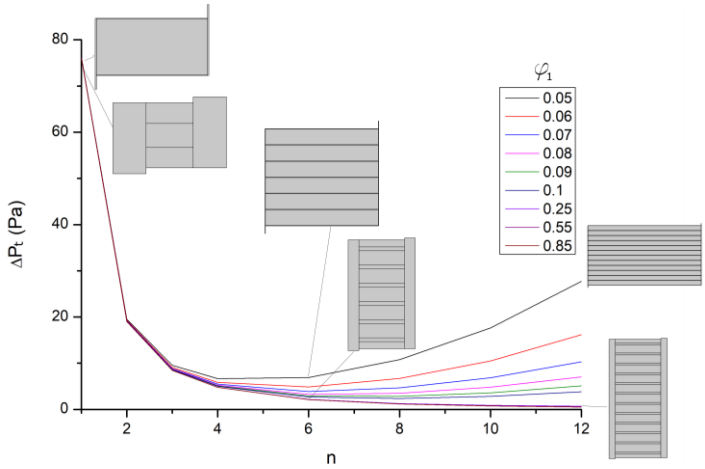

Figure 2 – Total pressure losses as a function of φ_1 and n, for K= 10^{-10} m².

Figure 2 shows that for $n \leq 3$, the effect of φ_1 in total pressure losses is negligible. We also see how for $\varphi_1 > 0.55$, minimum pressure losses are found by going in the direction of increasing number of elements in the construct, whereas for lower φ_1 values, there is no reason to increase n above 6. For $\varphi_1 \leq 0.07$, a point of minimum is found at n=6; For $\varphi_1 > 0.07$, negligible differences are found between n=6 and n=8; the same is true between $6 \leq n < 10$ for $\varphi_1 = 0.1$. Given a fixed value for n=6, the same conclusion presented previously is seen: the effect on total pressure losses is negligible when decreasing φ_1 to up to 0.07, below which it starts to increase.

3.1.2 Bed aspect ratio

Figure 3 shows how total pressure losses change when the number of elements in the construct also vary, and how the configuration of the first construct varies for both degrees of freedom.

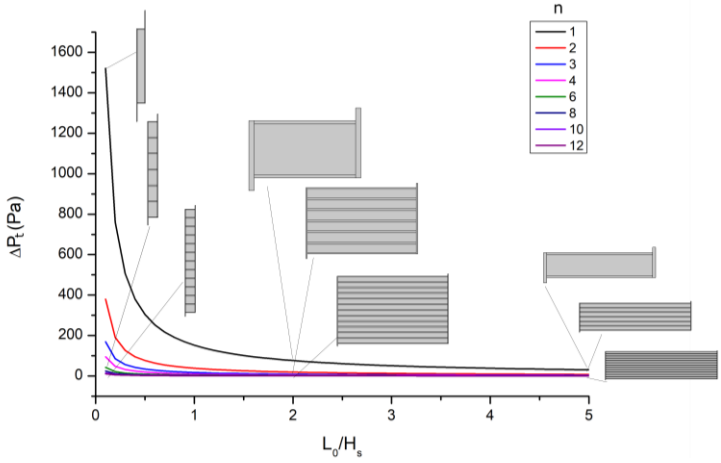

Figure 3 – Total pressure losses as a function of L_0/H_s and n, for K= 10^{-10} m².

The number of elements in the construct affects pressure losses in the bed for L_0/H_s <1 so that increasing n leads to lower pressure losses. However, for values of $L_0/H_s \geq 2$, pressure losses are constant and minimal for any n>1. Thus it is established the ratio $L_0/H_s \geq 2$ as desirable for design of the construct.

3.1.3 Width ratio of gas channels

The ratio between the width of L_0 and L_1 gas channels dictates the ratio of total pressure losses in free channels that occurs in one or the other types of channels. Based on the results for the previous DoF, the effect of this parameter on the pressure losses was studied for n=6, $\varphi = 0.2$ and $L_0/H_s = 2$. Results are presented in Figure 4.

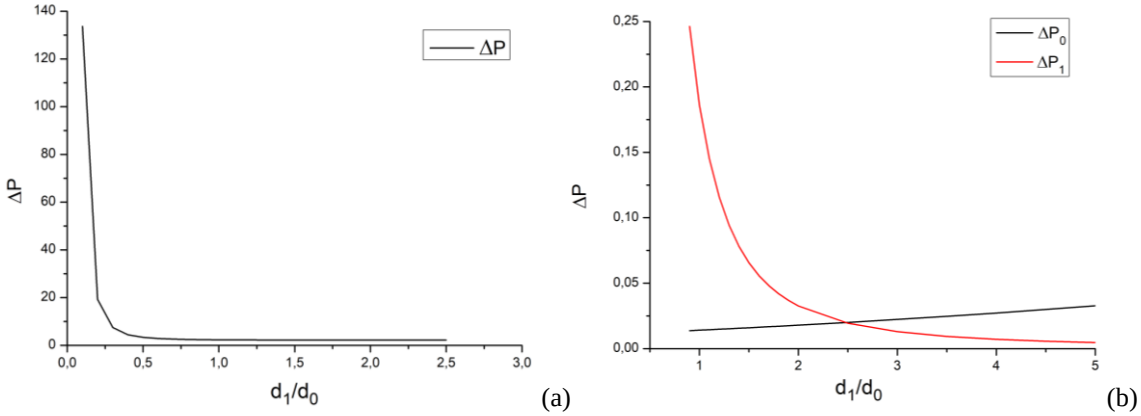

Figure 4– Total (a) and per component (b) pressure losses as a function of L_0/H_s, for n=6 and K= 10^{-10} m².

For this DoF, there is also a certain value (~2) above which it is possible to vary it freely without incurring in significant increase in total pressure losses. Figure b. shows how the minimum pressure losses are obtained, when the two terms (ΔP_0 and ΔP_1) are of the same order of magnitude, which is in accordance to the principle of equidistribution of imperfections.

4. NUMERICAL SIMULATION

A numerical simulation of the first construct, designed according to the Constructal method, was carried out in COMSOL Multiphysics® v. 5.3a, employing a 2D model based on the model and assumptions described above, for the conditions described in Table 3.

Table 3. Parameters and conditions for simulations

Parameter	Value	Design parameter	Value
Volumetric flow rate, Q (L/min)	50	Apparent porosity, φ	0.2
Inflow CO_2 concentration, CO_{2i} (mol/m³)	4.0393	L_0/H_s	2
Temperature, T (ºC)	80	d_1/d_0	2
Bed porosity, ε	0.47	Number of elements, n	6
Water volume fraction in pores, fw	0.2	Length of elemental volume, L_0 (m)	0.67
Diffusion coefficient of CO_2 in gas phase (mm²/s)	16	Elemental gas channel width, d_0 (m)	0.0052
		First construct height, L_1 (m)	0.37
		Bed height, d_s (m)	0.056

The procedure for numerical solution in software COMSOL Multiphysics® v. 5.3a consisted in solving mass transport equations in the free and porous medium, Navier-stokes equations for free flow in the gas channel, and Darcy's law for flor in the porous media. The boundary conditions employed were of an inlet velocity, outlet atmospheric pressure, no flux and no-slip at the internal walls, inflow CO_2 concentration, reaction in the porous bed and the transport properties.

A mesh convergence study was performed by varying the maximum mesh element size and keeping the other parameters equal to the defined by a physics defined mesh (configuration "Extra fine"), and the results were compared for a virtual probe at the reactor exit (position x=0.6778 m; y=0.37 m), measuring CO_2 concentration. Results for the study are presented in Figure 5.

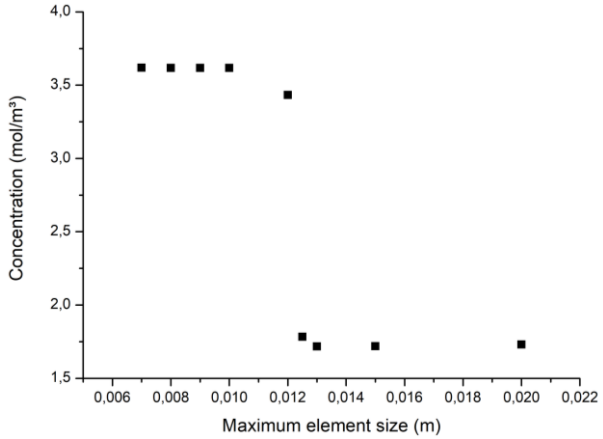

Figure 5– Mesh convergence study.

According to the results, it was adopted a value of 0.010 m for maximum element size of the mesh. The parameters of the mesh are presented in Table 3, and the geometry and mesh are presented in Figure 6.

Table 3. Mesh Parameters

Maximum element size (m)	0.010	Curvature factor	0.25
Minimum element size (m)	1.74E-4	Resolution of narrow regions	1
Maximum growth rate	1.1	Number of elements	27855

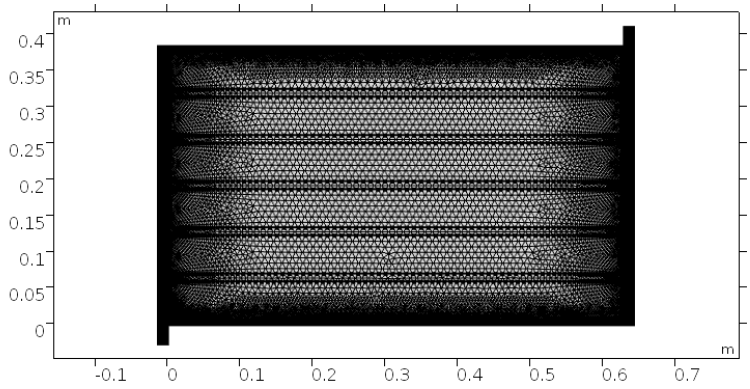

Figure 6. Geometry and mesh adopted for simulation

Results for the pressure and velocity profiles show a convergence to analytical results, as shown in Table.

Table 4. Comparison of Analytical and Numerical Results

Parameter	Analytical (average, length)	Numerical (average, surface)
Velocity in feeding channel, U_1 (m/s)	0.3799	0.40339
Velocity in elemental channel, U_0 (m/s)	0.1266	0.11023
Darcy velocity in porous bed, u (m/s)	0.002196	0.002149
Pressure losses, ΔP (Pa)	21.63	24.302

Figure 7 shows the velocity, dimensionless pressure (in relation to total pressure drop in the bed) and dimensionless concentration profiles in the first construct for n=6.

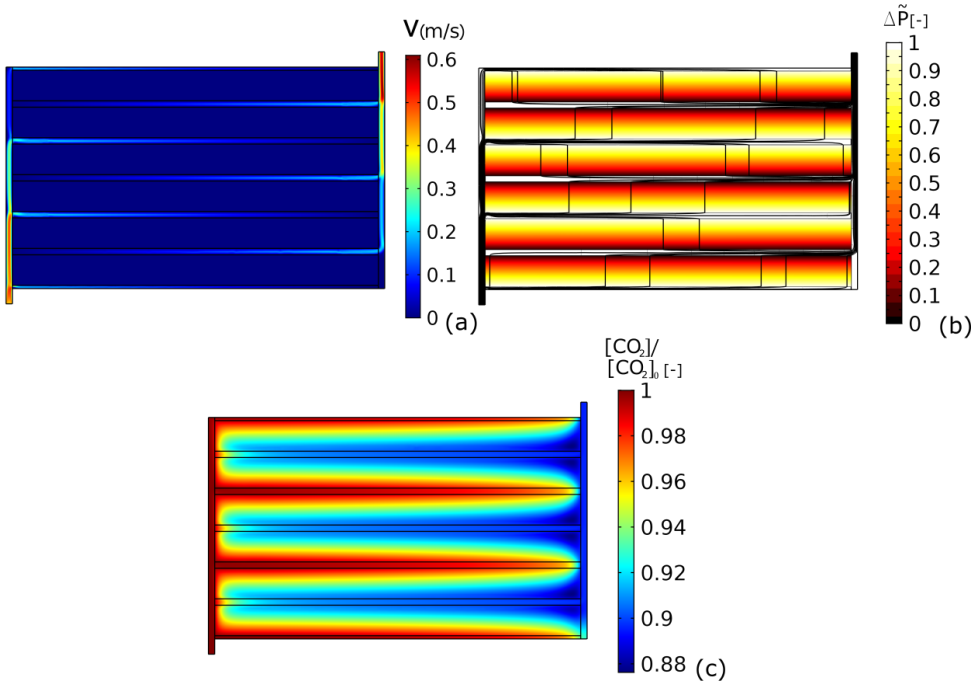

Figure 7. Numerical results for the first construct: a) Velocity (m/s); b) Dimensionless pressure; c) Dimensionless concentration profile

Results show that, for the preliminary designs explored in this study, the pressure drop in each bed is predominantly in the transversal direction of the bed, which may allow adequate simplifications in the model. For the designed reactor, it was possible to abate about 10.43% of CO_2 molar flow feeding stream for a relatively high flow rate (50 L/min) in a compact reactor (0.25 m²), in a total removal rate of 0.109 $kgCO_2.h^{-1}.m^{-3}$.

Results show that this design allows to carry out the process at ambient pressure for the considered parameters of flow rate and permeability of the medium, thus minimizing energy expenditure. However, the effect of inlet pressure on extent and kinetics of the carbonation reaction will be studied in future steps of the research.

5. CONCLUSIONS

The application of the Constructal method to a process of carbon dioxide capture with mineral carbonation made possible to obtain dimensioning guidelines for as well as the evolutionary path of geometry scales for the first construct of the process which minimize pressure losses.

Numerical results of removal in the porous bed showed good agreement with analytical results. The next steps in the research will continue to address the geometry problem for the device, searching optimal spacing distribution of higher constructs, with the goal of maximizing carbonation for a fixed reactor volume.

6. ACKNOWLEDGEMENTS

Financial assistance by ANEEL/COPEL P&D 2866-0470-2017 are gratefully acknowledged.
MRE work was partially supported by grant CNPq 312.615/2018-3 (Brazilian Federal Government).

7. REFERENCES

Bejan, A., and Lorente, S., 2008. *Design with Constructal Theory*. John Wiley & Sons, Hoboken, New Jersey.

Borgnakke, C., and Sonntag, R. E., 2013. *Fundamentals of Thermodynamics*. John Wiley & Sons, Hoboken, New Jersey.

Cecchi, E., Mouedhen, I., Kemache, N., Blais, J., and Mercier, G. (2017). "Effect of pCO_2 on direct flue gas mineral carbonation at pilot scale." Vol. 198, pp. 1–8.

Frank, M. J. W., Kuipers, J. A. M., and Van Swaaij, W. P. M., 1996. "Diffusion Coefficients and Viscosities of CO_2 + H_2O, CO_2 + CH_3OH, NH_3 + H_2O, and NH_3 + CH_3OH Liquid Mixtures." *J. Chem. Eng.*, Vol. 41, pp. 297–302.

Gasparovic, C. L. M., Froehner, S., Stanescu, G., and Errera, M. R., 2020. "Constructal Design of a Mineral Carbonation System for Post- Combustion Carbon Capture Energy." Proceedings of the 18th Brazilian Congress of Thermal Sciences and Engineering - ENCIT 2020. (Online), Brazil.

Gasparovic, C., Ostroski, A., Pedro, J., Vieira, B., and Risso, M., 2019. “Elementary Constructal Design of a carbon capture systems based on carbonation over fly ashes.” Vol., 37, pp. 2866.

Han, S. J., Yoo, M., Kim, D. W., and Wee, J. H., 2011. “Carbon dioxide capture using calcium hydroxide aqueous solution as the absorbent.” *Energy and Fuels*, Vol. 25, No. 8, pp. 3825–3834.

Ishida, T., and Maekawa, K., 2000. “Modeling of ph Profile in Pore Water Based on Mass Transport and Chemical Equilibrium Theory.” *Proceedings of JSCE, No.648/V-47*.

Jeong, J., Ramézani, H., and Chuta, E., 2019. “Reactive transport numerical modeling of mortar carbonation: Atmospheric and accelerated carbonation.” *Journal of Building Engineering*, Vol. 23, pp. 351–368.

Leung, D. Y. C., Caramanna, G., and Maroto-valer, M. M. (2014). “An overview of current status of carbon dioxide capture and storage technologies.” *Renewable and Sustainable Energy Reviews*, Vol. 39, pp. 426–443.

Li, M., Yang, H., Song, L., and Wu, Y., 2017. “Dynamic Coupling of Pore Structure Evolution with Carbonation Kinetics of CaO-Based Sorbents: Experiments and Modeling.” *Energy Fuels*, Vol. 31, pp. 12466-12476.

Malley-Ernewein, A., and Lorente, S.,2019. “Constructal design of thermochemical energy storage.” *International Journal of Heat and Mass Transfer*, Elsevier Ltd, 130, 1299–1306.

Mazzella, A., Errico, M., and Spiga, D., 2016. “CO_2 uptake capacity of coal fly ash: Influence of pressure and temperature on direct gas-solid carbonation.” *Journal of Environmental Chemical Engineering*, Vol. 4, No. 4, pp. 4120–4128.

Millignton, R. J., and Quirk, J. P., 1959. “Permeability of Porous Media.” *Nature*, Vol. 4658, pp. 387–388.

Mitchell, M. J., Jensen, O. E., Andrew Cliffe, K., and Mercedes Maroto-, M. (2010). “A model of carbon dioxide dissolution and mineral carbonation kinetics.” *Valer Source: Proceedings: Mathematical, Physical and Engineering Sciences*, Vol. 466, pp. 1265–1290.

Muriithi, G. N., Petrik, L. F., Fatoba, O., Gitari, W. M., Doucet, F. J., Nel, J., Nyale, S. M., and Chuks, P. E., 2013. “Comparison of CO2capture by ex-situ accelerated carbonation and in in-situ naturally weathered coal fly ash.” *Journal of Environmental Management*, Vol. 127, pp; 212–220.

Nield, D. A., and Bejan, A., 2017. *Convection in porous media*. Springer, ed., Cham, Switzerland.

Pan, S. Y., Chang, E. E., and Chiang, P. C., 2012. “CO2 capture by accelerated carbonation of alkaline wastes: A review on its principles and applications.” *Aerosol and Air Quality Research*, Vol. 12, No. 5, pp. 770–791.

Papadakis, V. G., Vayenas, C. G., and Fardis, M. N., 1989. “A reaction engineering approach to the problem of concrete carbonation.” *AIChE Journal*, Vol. 35, No. 10, pp. 1639–1650.

Rivera-Alvarez, A., and Bejan, A., 2003. “Constructal geometry and operation of adsorption processes.” *International Journal of Thermal Sciences*, Vol. 42, No. 10, pp. 983–994.

Sander, R., 2015. “Compilation of Henry’s law constants (version 4.0) for water as solvent.” *Atmospheric Chemistry and Physics*, Vol. 15, No. 8, pp. 4399–4981.

Siriruang, C., Toochinda, P., Julnipitawong, P., and Tangtermsirikul, S., 2016. “CO2capture using fly ash from coal fired power plant and applications of CO2-captured fly ash as a mineral admixture for concrete.” *Journal of Environmental Management*, Vol. 170, pp. 70–78.

Snoeyink, V., and Jenkins, D., 1980. *Water chemistry*. (J. W. & Sons, ed.), New York.

Ukwattage, N. L., Ranjith, P. G., and Li, X., 2017. “Steel-making slag for mineral sequestration of carbon dioxide by accelerated carbonation.” Vol., 97, pp. 15–22.

Ukwattage, N. L., Ranjith, P. G., Yellishetty, M., Bui, H. H., and Xu, T., 2015. “A laboratory-scale study of the aqueous mineral carbonation of coal fly ash for CO_2 sequestration.” *Journal of Cleaner Production*, Vol., 103, pp. 665–674.

8. RESPONSIBILITY NOTICE

The author(s) are the only responsible for the printed material included in this paper.